ACS OMEGA

http://pubs.acs.org/journal/acsodf

Article

Tailored Structure and Antibacterial Properties of Silica-Coated Silver Nanoplates by Pulsed Laser Irradiation

Emi Takeda,[⊥] Wei Xu,[⊥] Mitsuhiro Terakawa, and Takuro Niidome*

Cite This: *ACS Omega* 2022, 7, 7251−7256

Read Online

ACCESS | Metrics & More | Article Recommendations

ABSTRACT: We coated triangular-shaped silver nanoparticles, a type of anisotropic nanoplate (NPL), with silica (i.e., prepared Ag@SiO_2 NPLs). When we irradiated Ag@SiO_2 NPLs with nanosecond-pulsed laser light for 10 s, the triangular shape changed to spherical because of the photothermal effect. A high laser power exposed the silver core, and the particles exhibited strong antimicrobial activity. In contrast, at a moderate laser power, the silica layer crystallized, and the particles' antimicrobial activity decreased. Thus, a combination of Ag@SiO_2 NPLs and an appropriately tuned power of pulsed laser irradiation facilitated a decreased or an increased antimicrobial activity.

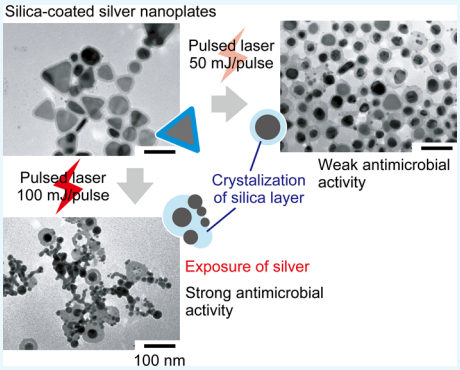

1. INTRODUCTION

Silver nanoparticles are a widely used antibacterial material, e.g., in textiles, housewares, food containers, and paints.[1] In medicine, silver nanoparticles are a broad-spectrum antimicrobial agent against several types of microbials—such as fungi, bacteria (including multidrug-resistant strains), and viruses.[2,3] Recently, researchers confirmed the antiviral activity of silver nanoparticles against severe acute respiratory syndrome coronavirus 2.[4] Although the mechanism of the antimicrobial activity remains to be fully elucidated, silver nanoparticles and free silver ions from the nanoparticles affect cell membranes and proteins. If silver nanoparticles and silver ions affect proteins that are involved in modulating intracellular redox activity, reactive oxygen species are induced, which kill the bacteria or suppress bacterial growth.[1,5]

Despite the antimicrobial activity, use of silver nanoparticles as antibacterial agents against infectious diseases is not common because silver nanoparticles are unstable and tend to form aggregates under physiological conditions in electrolytes, such as inorganic salts and proteins. Aggregation decreases the release of silver ions from the nanoparticles and reduces antibacterial activity at the site of infection. To improve the dispersion stability of silver nanoparticles, researchers have reported several surface modifications, e.g., polyethylene glycol (PEG),[6] poly-*N*-vinyl pyrrolidone,[6,7] proteins,[8] alginates,[9] chitosan,[10] and silica.[11]

We previously found that adding gold coatings onto silver nanoplates (NPLs) increased their dispersion stability.[12,13] However, coating with multiple gold layers hindered the NPLs' antibacterial activity. Thus, the gold coating turned the antibacterial activity to OFF. If we can change the core−shell structure of the gold-coated silver NPLs, resulting in release of silver ions, we can turn the antibacterial activity to ON. Accordingly, when we subjected gold-coated silver NPLs to pulsed laser irradiation that can heat the nanoparticles by the photothermal effect, the laser irradiation changed the nanoparticle shape from triangular to spherical. Concomitantly, silver ions were released from the nanoparticles and exhibited considerable antibacterial activity.[14] Thus, we switched the antibacterial activity from OFF to ON by laser irradiation. Zhu et al. also prepared gold-coated silver NPLs and enhanced silver ion release in response to laser irradiation. As a result, they observed antimicrobial activity and accelerated wound hearing in a mouse model.[15] Mei et al. prepared silver-coated gold nanorods. After irradiating them with laser light, the photothermal effect induced release of silver ions from the gold nanorods, which resulted in antibacterial activity and promoted would healing.[16] Gold−silver nanocages coated with silica also exhibit controlled release of silver ions and antibacterial activity by laser irradiation.[17] These on-demand activation systems of antibacterial activity of silver-containing nanoparticles will be an important basis of functional antimicrobial agents for medical applications with reduced side effects.

Received: December 14, 2021
Accepted: February 10, 2022
Published: February 18, 2022

In this study, we coated a silica layer instead of gold onto silver NPLs (i.e., Ag@SiO_2 NPLs), and we examined the effect of pulsed laser irradiation on their antimicrobial activity. We enhanced their antimicrobial activity by high-power pulse laser irradiation. At a moderate laser power, the antimicrobial activity decreased because of crystallization of the silica layer. Thus, a combination of Ag@SiO_2 NPLs and an appropriately tuned pulsed laser irradiation facilitated a decreased or an increased antimicrobial activity.

2. RESULTS AND DISCUSSION

2.1. Laser Irradiation of Silica-Coated Silver NPLs. Ag@SiO_2 NPLs displayed a major surface plasmon resonance peak at a wavelength of 660 nm, and their aqueous dispersed solution was blue (Figure 1). After pulsed laser irradiation of

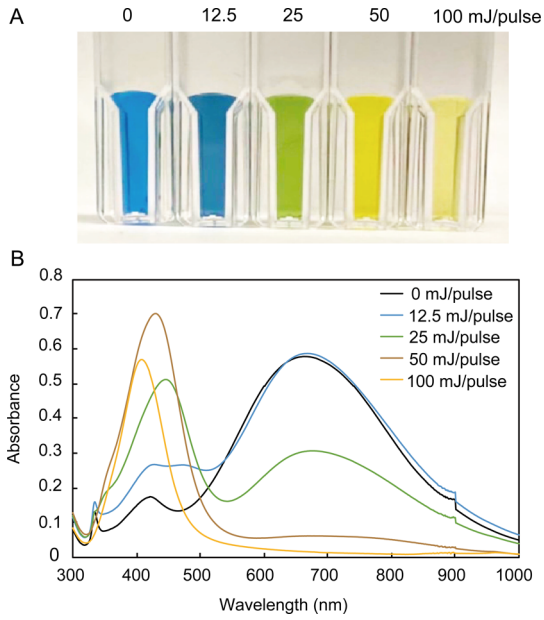

Figure 1. Change in color (A) and extinction spectra (B) of silica-coated silver nanoplates by pulsed laser irradiation.

Ag@SiO_2 NPLs, the color gradually changed from blue to yellow in accordance with increasing laser power. Concomitantly, the peak of the extinction spectrum shifted from a value of 660 nm to a value of 400 nm.

TEM observations confirmed the triangular shape of the Ag@SiO_2 NPLs before the laser irradiation, with an approximate diameter of 60 nm (Figure 2). After we irradiated the Ag@SiO_2 NPLs at 12.5 mJ/pulse for 10 s, we observed spherical particles. The rod-shaped particles might be vertically standing Ag@SiO_2 NPLs on the carbon membrane used for TEM observation. Regarding 25 and 50 mJ/pulse, most of the particles changed to a spherical form with a distinct silica layer. This shape change is similar to that observed in the gold-coated silver NPLs that we previously reported.[14] Thus, Ag@SiO_2 NPLs melted and changed to a spherical form because of the photothermal effect induced by pulsed laser irradiation. Since spherical silver nanoparticles generally show absorption at about 400 nm,[13,14] the color change to yellow shown in Figure 1 is consistent with the shape change to the spherical form by the laser irradiation. When we increased the laser power to 100 mJ/pulse, we observed small fragments of silver nanoparticles; the silica layer separated from the silver

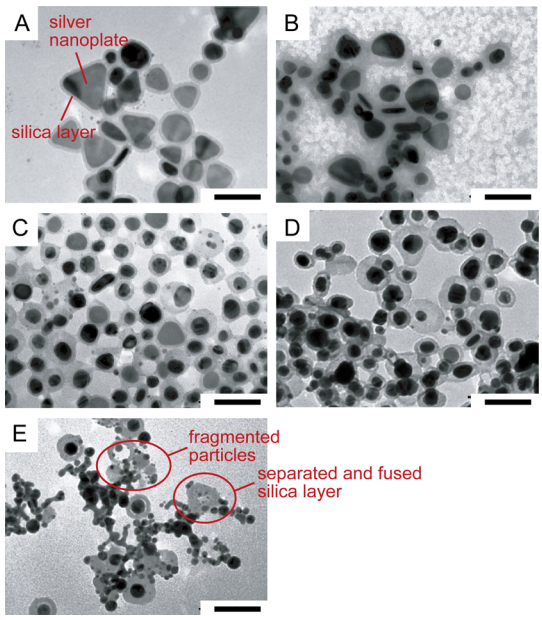

Figure 2. Shape changes of silica-coated silver nanoplates, indicated by transmission electron microscopy images acquired before and after pulsed laser irradiation: (A) before irradiation; (B)−(E), after irradiation at 12.5, 25, 50, and 100 mJ/pulse, respectively. Bars indicate 100 nm.

nanoparticles and tended to fuse with the silica layer of the adjoining particles. Production of the small fragments was attributable to laser ablation, which can be used for nanoparticle production from bulk metal.[18]

2.2. Change in Antibacterial Activity by Laser Irradiation. Next, we examined the antimicrobial activities of Ag@SiO_2 NPLs at 0.25 ppm before and after pulsed laser irradiation, tested using *S.* Typhimurium as a model microbe. Suppression of bacterial growth was 20% without pulsed laser irradiation, indicating that the Ag@SiO_2 NPLs exhibited moderate antibacterial activity (Figure 3). In our previous

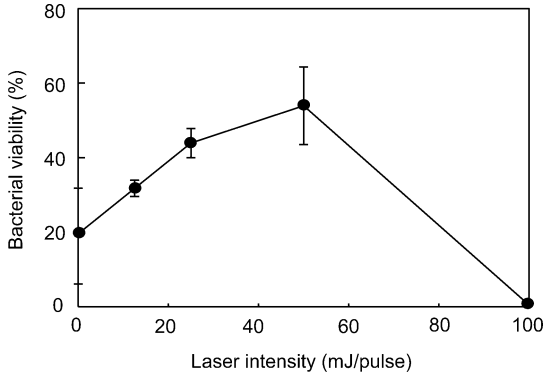

Figure 3. Antibacterial activity of Ag@SiO_2 nanoplates before and after pulsed laser irradiation at several laser powers. Data represent the mean value for n = 3, and bars are standard deviations of the means.

research, the silver NPLs without surface coating showed little antimicrobial activity because they form aggregates in bacterial culture.[12] The silica coating would improve the dispersion stability of the silver NPLs. When we irradiated Ag@SiO_2 NPLs at 12.5, 25, and 50 mJ/pulse, bacterial viability increased to 30, 40, and 50%, respectively. Thus, the antibacterial activity

https://doi.org/10.1021/acsomega.1c07058
ACS Omega 2022, 7, 7251−7256

of the Ag@SiO_2 NPLs decreased. Regarding 100 mJ/pulse, bacterial viability was 0% (we discuss these viability results in more detail in Section 2.3). The intense laser irradiation enhanced the antibacterial activity of Ag@SiO_2 NPLs. Thus, by increasing the power of the pulsed laser, the antibacterial activity of Ag@SiO_2 NPLs initially decreased and then increased, in accordance with increasing power.

Generally, the antibacterial activity of silver nanoparticles correlates with release of silver ions.[12−14] We next examined silver ion release from Ag@SiO_2 NPLs before and after pulsed laser irradiation. At 0.25 ppm of Ag@SiO_2 NPLs, the number of silver ions that were released from the Ag@SiO_2 NPLs before and after irradiation (12.5−100 mJ/pulse) was lower than the detection limit of inductively coupled plasma−optical emission spectroscopy. In the case of 40 ppm of Ag@SiO_2 NPLs, the concentration of released silver ions was ∼1 ppm (data not shown), indicating that ∼6 ppb of silver ions would be released from 0.25 ppm of Ag@SiO_2 NPLs. The release was insufficient to exhibit antimicrobial activity against *S.* Typhimurium.[12] Therefore, direct interaction of Ag@SiO_2 NPLs was the cause of bacterial death. When we observed a mixture of the irradiated Ag@SiO_2 NPLs and *S.* Typhimurium with a TEM, many of the original (i.e., before light irradiation) and irradiated Ag@SiO_2 NPLs were bound to the bacteria (Figure 4).

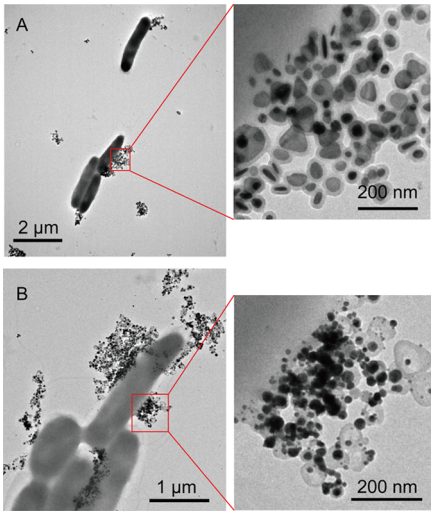

Figure 4. Transmission electron microscopy images of mixtures of bacteria (*S.* Typhimurium) and Ag@SiO_2 nanoplates: (A) before and (B) after irradiation at 100 mJ/pulse.

The TEM image of Ag@SiO_2 NPLs after laser irradiation at 100 mJ/pulse (Figure 2E) indicates that the silica layer separated from the fragmented silver nanoparticles. Next, we performed X-ray photoelectron spectroscopy (XPS) analysis to clarify the exposure of silver atoms from the core of the Ag@SiO_2 NPLs. The original Ag@SiO_2 NPLs (i.e., before laser irradiation) exhibited only the signal of O1s (533 eV), Si2s (155 eV), and Si2g (104 eV) (Figure 5A). Signals from Ag [Ag3p (604 and 573 eV), $Ag3d^3$ (374 eV), and $Ag3d^5$ (368 eV)] were faint, indicating that the silica layers were fully coated on the silver NPLs. When we irradiated the Ag@SiO_2 NPLs, the signal from the Ag linearly increased with increasing laser power. We could not explain the reduced antimicrobial activity at 50 mJ/pulse from this result; however, the strong antimicrobial activity after irradiation at 100 mJ/pulse may be

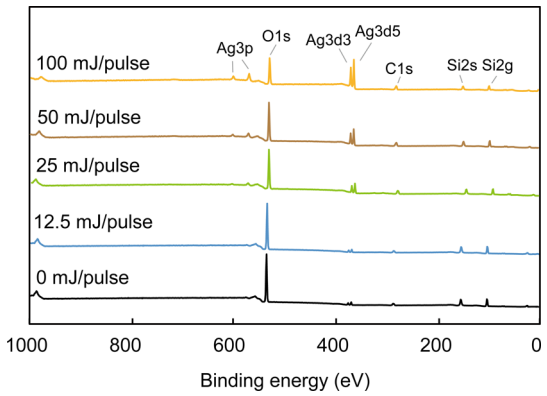

Figure 5. XPS survey spectrum of silica-coated silver nanoplates before and after pulsed laser irradiation.

because of exposure of the silver by laser irradiation: by combining the fragmentation of the silver nanoparticles with direct interaction of the silver with the bacteria.

2.3. Crystallization of Silica Layers. The silica layer fabricated by the Stöber process on the silver NPLs is in the amorphous state.[19] Generally, amorphous silica can be converted to the crystalline state (quartz) by heating above 800 °C.[20] In the previous section, we mentioned that the silver NPLs changed their shape to spherical because of the photothermal effect by laser irradiation that melted the nanoparticles. The melting temperature of silver is 962 °C, indicating that we heated the silica layers on the silver nanoparticles beyond the melting temperature. Therefore, we hypothesize that the temperature increase that is attributable to the photothermal effect may have induced crystallization of the amorphous silica to quartz; as a result, the antimicrobial activity decreased at moderate laser power (12.5−50 mJ/pulse). To confirm crystallization of amorphous silica, we acquired FTIR spectra of Ag@SiO_2 NPLs before and after laser irradiation (Figure 6). The original Ag@SiO_2 NPLs (i.e., before laser irradiation) exhibited a broad absorption band at ∼3500 cm^{-1}, which we assigned to the stretching vibration of the hydroxy group in amorphous silica. After laser irradiation, the absorption band decreased. Thus, laser irradiation converted the Si−OH in amorphous silica to Si−O−Si, which is the unit of crystalline quartz. Thus, we confirmed the crystallization of the silica layer that corresponds to the antimicrobial activity of the silver nanoparticles.

From these results, we conclude that laser irradiation at moderate power suppressed the antimicrobial activity of Ag@SiO_2 NPLs; however, antimicrobial activity can be activated by a stronger power of laser irradiation. Thus, we can tune the laser power in a manner that modulates the antimicrobial activity of the silver NPLs (i.e., a decrease or an increase). In our previous study, we succeeded in OFF-to-ON control of the antimicrobial activity of gold-coated silver NPLs by using a gold coating.[14] Here, the silica layer exhibited unique structural changes by the photothermal effect of Ag@SiO_2 NPLs—from amorphous to crystalline—and separation from the silver particles. This unique property of the silica layer provides researchers with an additional means of modulating the antibacterial activity of silver nanoparticles.

Pulsed lasers emit an extremely high energy in an extremely short time. When we irradiated the Ag@SiO_2 NPLs with a pulsed laser, they were heated by the photothermal effect, then melted, deformed to a spherical shape, and fragmented. This is

https://doi.org/10.1021/acsomega.1c07058
ACS Omega 2022, 7, 7251−7256

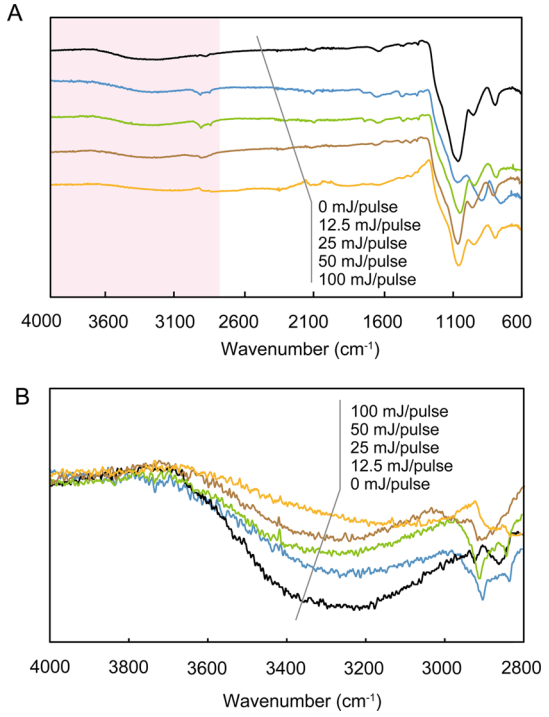

Figure 6. (A) FTIR spectra of Ag@SiO_2 nanoplates before and after pulsed laser irradiation. (B) Enlarged spectra from 4000 to 2800 cm^{-1}.

a unique characteristic of anisotropic metallic nanoparticles.[14,21,22] In this process, the local temperature increased to ∼1000 °C, exceeding the melting point of silver nanoparticles, and corresponding to the conversion of amorphous silica to crystalline quartz. After the shape change to a spherical form, there was no more absorption at 532 nm (Figure 1B). Thus, the heating stopped after the shape change, and the ambient temperature of the aqueous solution did not increase (data not shown). This is the first report (to the best of our knowledge) of conversion of amorphous silica to crystalline quartz in aqueous solution. It will be a fundamental technique for preparing nanosized quartz, a novel nanostructure that can be used for medical and industrial use.

3. CONCLUSIONS

We coated silver NPLs with a silica layer and irradiated them with nanosecond-pulsed laser light for 10 s. The color of the silver nanoparticles changed from blue to yellow, and their triangular shape changed to spherical. At the high laser power (100 mJ/pulse), some of the silver nanoparticles fragmented, the silica layer tended to fuse with that of the adjoining particles, and the silver core was exposed to the particle surface. As a result, the antimicrobial activity was enhanced. In contrast, at moderate laser power (12.5−50 mJ/pulse), the antimicrobial activity was reduced. The laser irradiation heated the silica layer by the photothermal effect of the silver NPLs and crystallized the silica layer. Crystallization of the silica layer without exposure of the silver core suppressed the antimicrobial activity. Thus, a combination of Ag@SiO_2 NPLs and pulsed laser irradiation enabled us to decrease or increase the antimicrobial activity by modulating the laser power. As applications of this system, it will be a functional antibacterial agent for intractable infectious diseases, e.g., tuberculosis caused by *Mycobacterium tuberculosis*, intracellular parasite, where the antimicrobial agent has to show activity only in infected cells without showing any cytotoxicity against healthy cells. It will also be applied to prepare a bacterial pattern that can be drawn by laser irradiation to examine bacterial cell−cell communications. In addition, we have presented a fundamental technique to prepare nanosized quartz as a novel nanostructure.

4. EXPERIMENTAL METHODS

4.1. Chemicals. Trisodium citrate, sodium borohydride, *L*(+)-ascorbic acid, tryptone, dried yeast extract, sodium chloride, and agar powder were purchased from Nakarai Tesque (Kyoto, Japan). Poly(*p*-styrenesulfonic acid) solution, silver nitrate, ammonia aqueous solution (28 wt %), and ethanol (99.5 wt %) were purchased from FUJIFILM Wako Pure Chemical Industries (Osaka, Japan). Thiol-terminated PEG (PEG−SH; 5000 Da) was purchased from NOF Co., Ltd. (Tokyo, Japan). Tetraethyl orthosilicate (TEOS) was purchased from Tokyo Chemical Industry Co., Ltd. (Tokyo, Japan).

4.2. Preparation of Silver NPLs and Silica Coating. Silver NPLs were prepared in two steps.[23,24] Briefly, a seed solution of silver nanoparticles was first prepared. Then, 20 mL of 2.5 mM sodium citrate, 1 mL of 0.5 g/L polystyrene sulfonate, and 1.2 mL of 10 mM $NaBH_4$ were mixed in a conical flask with continuous stirring. Next, 50 mL of 0.5 mM $AgNO_3$ was added at a rate of 20 mL/min. With continuous stirring, the solution was allowed to stand for 60 min at 30 °C.

For preparing silver NPLs, 1 mL of the prepared seed solution of silver nanoparticles was mixed with 200 mL of distilled water and 4.5 mL of 10 mM ascorbic acid. Then, with continued stirring, 120 mL of 0.5 mM $AgNO_3$ was added at a rate of 30 mL/min, and stirring continued for 4 min. Next, 20 mL of 25 mM sodium citrate was added. The prepared solution was allowed to stand at 30 °C for 100 h.

Ag@SiO_2 NPLs were then prepared.[21] Briefly, the Ag NPL solution was centrifuged at 13,420× *g* for 15 min, decanted, and resuspended in Milli-Q water. To a total of 10 mL of a solution of 0.223 mM Ag NPLs (concentration based on silver atoms), 1 mL of 0.5 mM PEG−SH was added. After stirring for 3 h, an additional 0.5 mL of 0.5 mM PEG−SH was added and the mixture was stirred at room temperature for 21 h. The PEG-modified Ag NPLs were coated with a silica layer by a modified Stöber process based on hydrolysis of TEOS in an ethanol/water mixture in the presence of Ag NPLs. A solution of the prepared PEG-modified Ag NPLs was concentrated by centrifugation at 13,420× *g* for 15 min. A total of 1 mL of a solution of 0.223 mM PEG-modified Ag NPLs (based on silver atoms) was diluted with 7.7 mL of ethanol. The mixture was added to 200 μL of 5 wt % ammonia, and 1.1 mL of 45 mM TEOS was then added. The mixture was stirred for 48 h and then centrifuged at 13,420× *g* for 15 min, decanted, and resuspended in an ethanol/water solution (9/1 v/v) to remove excess ammonia and TEOS.

4.3. Characterizations. The shape and size of the Ag@SiO_2 NPLs were observed with a transmission electron microscope (TEM; JEM-1400plus; JEOL, Japan). The absorption spectra were characterized with a UV−vis−near-IR spectrophotometer (V-670; Jasco, Tokyo, Japan). Silver ions released from the silver nanoparticles were evaluated by inductively coupled plasma−optical emission spectroscopy (Thermo iCAP 7000 Series ICP; Thermo Fisher Scientific, Waltham, MA, USA). Elemental analysis of the nanoparticles

https://doi.org/10.1021/acsomega.1c07058
ACS Omega 2022, 7, 7251−7256

was performed by XPS (Theta Probe; Thermo Fisher Scientific, Waltham, MA, USA) with monochromatic Al Kα irradiation. The crystallization of the silica layer was evaluated with an FTIR spectrophotometer (FT/IR-4200; Jasco, Tokyo, Japan).

4.4. Laser Irradiation. After preparing the Ag@SiO_2 NPLs, they were subjected to pulsed laser irradiation and their characteristics were examined, i.e., absorbance spectra and TEM observations, antimicrobial activity, and silver ion release. A pulsed laser can produce a high peak power compared with a continuous-wave laser. One hundred fifty microliters of Ag@SiO_2 NPLs were aliquoted into a 96-well glass bottom plate. Six-nanosecond (full width at half maximum) laser pulses emitted from the pulsed laser were reflected by plane mirrors to irradiate the sample from the top side. The beam diameter of the laser pulse was 6 mm. Irradiation was carried out with the second harmonics (532 nm) of a Q-switched Nd:YAG laser at a repetition rate of 10 Hz. The irradiation time was 10 s with laser energies of 12.5, 25, 50, and 100 mJ/pulse. The laser energy transferable to the NPL was determined by the incident laser energy and the absorbance. Therefore, although the absorbance at 532 nm was only approximately half that at 660 nm, the laser was sufficient to obtain an appropriate laser energy; the sufficiency of this laser energy was also confirmed by our experiments indicating the change in shape to a spherical form. The irradiated nanoparticles were used in measurements of antimicrobial activity, TEM observation, and other analyses.

4.5. Antimicrobial Activity. The antibacterial properties of Ag@SiO_2 NPLs before and after pulsed laser irradiation were examined by turbidity. To prepare Ag@SiO_2 NPL samples for testing, Ag@SiO_2 NPLs were centrifuged at 13,420× *g* for 15 min at 25 °C. The supernatant was removed, and the pellet was redispersed in ultrapure water to remove silver ions spontaneously released from the Ag@SiO_2 NPLs. *Salmonella enterica serovar* Typhimurium (*S.* Typhimurium; LT-2 strain) that had been stocked in glycerol at −80 °C was spread onto lysogeny broth (LB) agar plates, and incubated at 37 °C overnight to produce colonies. A single colony of *S.* Typhimurium was inoculated into the liquid LB medium and cultured at 37 °C overnight. The medium was further diluted 100-fold with a fresh liquid LB medium and cultured for 4 h. This medium was diluted 10,000× and used as a medium for antibacterial activity tests. Next, 200 μL of *S.* Typhimurium culture solution and 50 μL of silica-coated silver NPL aqueous dispersion were mixed in 96-well microplate wells at 0.25 ppm and incubated at 37 °C for 9 h. Then, the antibacterial activity was evaluated by measuring the absorbance at 620 nm with a microplate reader (Infinite F50; TECAN, Switzerland). The experiment was performed in triplicate, and the data were expressed as mean ± standard deviation (n = 3).

4.6. TEM Observation of Ag@SiO_2 NPL Binding on *S.* Typhimurium. Ag@SiO_2 NPLs (50 μLof 50 μg/mL) were added to 200 μL of *S.* Typhimurium and cultured for 30 min. Then, the suspension was dropped onto a TEM grid and allowed to stand for 2 min. After removing the excess suspension, fixation with 4% paraformaldehyde for 5 min was followed by dehydration in gradient ethanol solutions (25, 50, 75, 90, and 100%) for 3 min. The grid was observed under TEM at 80 kV.

AUTHOR INFORMATION

Corresponding Author

Takuro Niidome − *Faculty of Advanced Science and Technology, Kumamoto University, Kumamoto 860-8555, Japan;* orcid.org/0000-0002-8070-8708; Email: niidome@kumamoto-u.ac.jp

Authors

Emi Takeda − *Faculty of Advanced Science and Technology, Kumamoto University, Kumamoto 860-8555, Japan*

Wei Xu − *Faculty of Advanced Science and Technology, Kumamoto University, Kumamoto 860-8555, Japan*

Mitsuhiro Terakawa − *School of Integrated Design Engineering and Department of Electronics and Electrical Engineering, Keio University, Yokohama 223-8522, Japan;* orcid.org/0000-0001-9526-7039

Complete contact information is available at: https://pubs.acs.org/10.1021/acsomega.1c07058

Author Contributions

$^{\perp}$E.T. and W.X. contributed equally to this study. E.T. prepared the silica-coated silver nanoplates and performed measurement of absorption spectra and TEM observation. W.X. performed TEM observation, measurement of XPS, and FTIR. M.T. performed the laser irradiation. The manuscript was prepared through contributions from all authors.

Funding

This research was funded by Japan Science and Technology Agency (JST), Core Research for Evolutional Science and Technology (CREST) (Grant Number JPMJCR18H5).

Notes

The authors declare no competing financial interest.

ACKNOWLEDGMENTS

This research was funded by the Japan Science and Technology Agency (JST), Core Research for Evolutional Science and Technology (CREST) (Grant Number JPMJCR18H5). We thank Mr. Kei Ohori and Prof. Shintaro Ida for help with the FTIR and XPS measurements and data analyses. We also thank Michael Scott Long, PhD, from Edanz (https://jp.edanz.com/ac) for editing a draft of this manuscript.

ABBREVIATIONS

Ag@SiO_2 NPLs, silica-coated Ag NPLs; TEM, transmission electron microscope; XPS, X-ray photoelectron spectroscopy

REFERENCES

(1) Hajipour, M. J.; Fromm, K. M.; Ashkarran, A. A.; Aberasturi, D. J.; Larramendi, I. R.; Rojo, T.; Serpooshan, V.; Parak, W.; Mahmoudi, M. Antibacterial Properties of Nanoparticles. *Trends Biotechnol.* **2012**, *30*, 499−511.

(2) Chopra, I. The Increasing Use of Silver-Based Products as Antimicrobial Agents: a Useful Development or a Cause for Concern? *J. Antimicrob. Chemother.* **2007**, *59*, 587−590.

(3) Zhang, X. F.; Liu, Z. G.; Shen, W.; Gurunathan, S. Silver Nanoparticles: Synthesis, Characterization, Properties, Applications, and Therapeutic Approaches. *Int. J. Mol. Sci.* **2016**, *17*, 1534.

(4) Jeremiah, S. S.; Miyakawa, K.; Morita, T.; Yamaoka, Y.; Ryo, A. Potent antiviral effect of silver nanoparticles on SARS-CoV-2. *Biochem. Biophys. Res. Commun.* **2020**, *533*, 195−200.

https://doi.org/10.1021/acsomega.1c07058
ACS Omega 2022, 7, 7251−7256

(5) Yan, X.; He, B.; Liu, L.; Qu, G.; Shi, J.; Hu, L.; Jiang, G. Antibacterial Mechanism of Silver Nanoparticles in *Pseudomonas aeruginosa*: Proteomics Approach. *Metallomics* **2018**, *10*, 557−564.
(6) Tejamaya, M.; Römer, I.; Merrifield, R. C.; Lead, J. R. Stability of Citrate, PVP, and PEG Coated Silver Nanoparticles in Ecotoxicology Media. *Environ. Sci. Technol.* **2012**, *46*, 7011−7017.
(7) Huynh, K. A.; Chen, K. L. Aggregation Kinetics of Citrate and Polyvinylpyrrolidone Coated Silver Nanoparticles in Monovalent and Divalent Electrolyte Solutions. *Environ. Sci. Technol.* **2011**, *45*, 5564−5571.
(8) Gebauer, J. S.; Malissek, M.; Simon, S.; Knauer, S. K.; Maskos, M.; Stauber, R. H.; Peukert, W.; Treuel, L. Impact of the Nanoparticle−Protein Corona on Colloidal Stability and Protein Structure. *Langmuir* **2012**, *28*, 9673−9679.
(9) Liu, Y.; Chen, S.; Zhong, L.; Wu, G. Preparation of High-Stable Silver Nanoparticle Dispersion by Using Sodium Alginate as a Stabilizer Under Gamma Radiation. *Radiat. Phys. Chem.* **2009**, *78*, 251−255.
(10) Boca, S. C.; Potara, M.; Gabudean, A. M.; Juhem, A.; Baldeck, P. L.; Astilean, S. Chitosan-Coated Triangular Silver Nanoparticles as a Novel Class of Biocompatible, Highly Effective Photothermal Transducers for in Vitro Cancer Cell Therapy. *Cancer Lett.* **2011**, *311*, 131−140.
(11) Brandon, M. P.; Ledwith, D. M.; Kelly, J. M. Preparation of Saline-Stable, Silica-Coated Triangular Silver Nanoplates of Use for Optical Sensing. *J. Colloid Interface Sci.* **2014**, *415*, 77−84.
(12) Ichimaru, H.; Harada, A.; Yoshimoto, S.; Miyazawa, Y.; Mizoguchi, D.; Kyaw, K.; Ono, K.; Tsutsuki, H.; Sawa, T.; Niidome, T. Gold Coating of Silver Nanoplates for Enhanced Dispersion Stability and Efficient Antimicrobial Activity against Intracellular Bacteria. *Langmuir* **2018**, *34*, 10413−10418.
(13) Harada, A.; Ichimaru, H.; Kawagoe, T.; Tsushida, M.; Niidome, Y.; Tsutsuki, H.; Sawa, T.; Niidome, T. Gold-Treated Silver Nanoparticles Have Enhanced Antimicrobial Activity. *Bull. Chem. Soc. Jpn.* **2019**, *92*, 297−301.
(14) Kyaw, K.; Ichimaru, H.; Kawagoe, T.; Terakawa, M.; Miyazawa, Y.; Mizoguchi, D.; Tsushida, M.; Niidome, T. Effects of Pulsed Laser Iradiation on Gold-Coated Silver Nanoplates and Their Antibacterial Activity. *Nanoscale* **2017**, *9*, 16101−16105.
(15) Zhu, J.; Liu, S.; Zhang, T.; Zhang, Y.; Zhang, X.; Liu, X.; Tie, Z.; Dou, Y.; Lu, Z.; Hu, Y. Porous Gold Layer Coated Silver Nanoplates with Efficient Antimicrobial Activity. *Colloids Surf., B* **2020**, *186*, No. 110727.
(16) Mei, Z.; Gao, D.; Hu, D.; Zhou, H.; Ma, T.; Huang, L.; Liu, X.; Zheng, R.; Zheng, H.; Zhao, P.; Zhou, J.; Sheng, Z. Activatable NIR-II Photoacoustic Imaging and Photochemical Synergistic Therapy of MRSA Infections Using Miniature Au/Ag Nanorods. *Biomaterials* **2020**, *251*, No. 120092.
(17) Wu, S.; Li, A.; Zhao, X.; Zhang, C.; Yu, B.; Zhao, N.; Xu, F.-J. Silica-Coated Gold−Silver Nanocages as Photothermal Antibacterial Agents for Combined Anti-Infective Therapy. *ACS Appl. Mater. Interfaces* **2019**, *11*, 17177−17183.
(18) Fazio, E.; Gökce, B.; Giacomo, A. D.; Meneghetti, M.; Compagnini, G.; Tommasini, M.; Waag, F.; Lucotti, A.; Zanchi, C. G.; Ossi, P. M.; Dell'Aglio, M.; D'Urso, L.; Condorelli, M.; Scardaci, V.; Biscaglia, F.; Litti, L.; Gobbo, M.; Gallo, G.; Santoro, M.; Trusso, S. Nanoparticles Engineering by Pulsed Laser Ablation in Liquids: Concepts and Applications. *Nanomaterials* **2020**, *10*, 2317.
(19) Stöber, W.; Fink, A.; Bohn, E. Controlled Growth of Monodisperse Silica Spheres in the Micron Size Range. *J. Colloid Interface Sci.* **1968**, *26*, 62−69.
(20) Bertoluzza, A.; Fagnano, C.; Morelli, M. A.; Gottardi, V.; Guglielmi, M. Raman and Infrared Spectra on Silica gel Evolving Toward Glass. *J. Non-Cryst. Solids* **1982**, *48*, 117−128.
(21) Tang, H.; Kobayashi, H.; Niidome, Y.; Mori, T.; Katayama, Y.; Niidome, T. CW/Pulsed NIR Irradiation of Gold Nanorods: Effect on Transdermal Protein Delivery Mediated by Photothermal Ablation. *J. Controlled Release* **2013**, *171*, 178−183.
(22) Niidome, Y.; Haine, A. T.; Niidome, T. Anisotropic Gold-Based Nanoparticles: Preparation, Properties, and Applications. *Chem. Lett.* **2016**, *45*, 488−498.
(23) Gao, C.; Lu, Z.; Liu, Y.; Zhang, Q.; Chi, M.; Cheng, Q.; Yin, Y. Highly Stable Silver Nanoplates for Surface Plasmon Resonance Biosensing. *Angew. Chem., Int. Ed.* **2012**, *51*, 5629−5633.
(24) Aherne, D.; Ledwith, D. M.; Gara, M.; Kelly, J. M. Optical Properties and Growth Aspects of Silver Nanoprisms Produced by a Highly Reproducible and Rapid Synthesis at Room Temperature. *Adv. Funct. Mater.* **2008**, *18*, 2005−2016.

https://doi.org/10.1021/acsomega.1c07058
ACS Omega 2022, 7, 7251−7256